TCABSE-J Research Article

ISSN: 2583- 2557, *Volume 1, Issue 5, pp1-11. 2023.*

TCABSE-J Interdisciplinary Sciences Journal

In silico analysis of molnupiravir usage vs. efficacy of COVID-19 vaccines.

Madhuri Vissapragada[1, 2, #], Santhinissi Addala[1, 3, #], Madhumita Aggunna[1], Niharikha Mukala[1], Jahnavi Chintalapati[1, 3], Akhila Kamidi[1], Meghana S. Korabu[1, 4], Manisha Lanka[1], Hemsai Palla[1, 5], Manikanta Sodasani[1], Abhinav V.K.S. Grandhi[1, 6], Afeez Unnisa[1], Alekhya Adhikari[1, 5], Ayyappa D. Kumpatla[1, 7], Bhagyasri Yerabolu[1, 7], Chamanthi Paidi[1, 5], Gayathri Pemmadi[1, 5], Hanisha Penta[1, 8], Hemasri Mallavalli[1, 5], Kamalakumari Gadigoyala[1, 9], Mahalakshmi Voleti[1, 9], Maheswari Ravilisetty[1], Neelimadevi Akula[1, 8], Prathyusha Gundubogula[1, 2], Prathyusha Puripanda[1, 2], Pravallika Lankapalli[1, 3], Pravallika Sandipamu[1, 9], Rakshita Nagraj[10], Ramya Tamarala[1, 9], Ratnapriya Geddam[6], Raviteja Kolluru[1, 11], Raviteja Oggu[1, 12], Roopini Garbhapu[1, 3], Saitejasri Meka[1, 2], Sathvika Geddam[1, 5], Sowjanya Viyyapu[1, 2], Sowmya Sammangi[1, 5], Sravanalakshmi Javvaji[1, 13], Srinjoy Chattopadhyay[14], Srividya Inemella[1, 11], Vasavi Grandhi[1], Yathiraj Chigilipalli[1, 9], Yuktha C. Puppala[1, 2], Madhura H. Sharma[15], Sravyasree Gubbala[1, 16], Kajalkumari Thakur[1], Saimythely Anaparthi[17], Bhashmika R. Pothula[17] and Ravikiran S. Yedidi[1, 9, *]

[1]Department of Intramural research core, The Center for Advanced-Applied Biological Sciences & Entrepreneurship (TCABS-E), Visakhapatnam 530016, A.P. India; [2]Department of Human Genetics, Andhra University, Visakhapatnam 530003, A.P. India; [3]Department of Biochemistry, Andhra University, Visakhapatnam 530003, A.P. India; [4]Department of Biotechnology, Dr. Lankapalli Bullayya College, Visakhapatnam 530013, A.P. India; [5]Department of Biotechnology, Andhra University, Visakhapatnam 530003, A.P. India; [6]Koringa College of Pharmacy, Korangi 533461, A.P. India; [7]Department of Pharmacognosy, Andhra University, Visakhapatnam 530003, A.P. India; [8]Department of Microbiology, Andhra University, Visakhapatnam 530003, A.P. India; [9]Department of Zoology, Andhra University, Visakhapatnam 530003, A.P. India; [10]Department of Biotechnology, BMS College for Women, Bengaluru 560004, K.A. India; [11]Department of Pharmaceutical Biotechnology, Andhra University, Visakhapatnam 530003, A.P. India; [12]Department of Pharmaceutical Chemistry, Andhra University, Visakhapatnam 530003, A.P. India; [13]Department of Pharmacology, Andhra University, Visakhapatnam 530003, A.P. India; [14]Department of Biology and Biotechnology, The University of Pavia, Pavia, Italy; [15]Department of Molecular Biology, University of Mysore Yuvaraja's College, Mysuru 570005, K.A. India; [16]Amrita Vishwa Vidyapeetham, Amritapuri 690525, K.L. India; [17]Department of Chemical Engineering, Andhra University, Visakhapatnam 530003, A.P. India. (#These authors contributed equally; *Correspondence to R.S.Y.: tcabse.india@gmail.com)

Due to the emerging variants of Severe Acute Respiratory Syndrome Coronavirus type-2 (SARS CoV-2), the causative virus of coronavirus disease-2019 (COVID-19), the efficacy of vaccines against COVID-19 is severely challenged. Additionally, certain chemotherapeutic antiviral agents may worsen this global health issue even more. Molnupiravir is an antiviral agent approved for COVID-19 treatment that works by incorporating itself into the viral RNA causing severe mutagenesis and lethality to SARS CoV-2. In this study we hypothesized that if such severely mutated variants of SARS CoV-2 were to survive and replicate then the surface topology of these mutant viral spike proteins (antigen) would be altered thus challenging the antibodies generated from the current vaccine administrations. In order to address this hypothesis, we performed a systematic *in silico* analysis of all the possible mutant variants that can be generated by molnupiravir and evaluated the possible risks that they can cause to the current vaccines. Our results suggest that the mutant viral variants generated due to the incorporation of molnupiravir may cause low to severe damage to the efficacy of current vaccines due to the altered structure of the mutant viral spike protein models. The outcome of this study should be considered in the future vaccine design so that a co-administration of molnupiravir along with vaccination may result in a synergy rather than a catastrophe.

Keywords: COVID-19, SARS CoV-2, Molnupiravir, vaccines, efficacy, mutations, antigen, epitope.

Citation: Vissapragada, M., Addala, S., Aggunna, M., Mukala, N., Chintalapati, J., Kamidi, A., Korabu, M. S., Lanka, M., Palla, H., Sodasani, M., Grandhi, A. V. K. S., Unnisa, A., Adhikari, A., Kumpatla, A. D., Yerabolu, B., Paidi, C., Pemmadi, G., Penta, H., Mallavalli, H., Gadigoyala, K., Voleti, M., Ravilisetty, M., Akula, N., Gundubogula, P., Puripanda, P., Lankapalli, P., Sandipamu, P., Nagraj, R., Tamarala, R., Geddam, R., Kolluru, R., Oggu, R., Garbhapu, R., Meka, S., Geddam, S., Viyyapu, S., Sammangi, S., Javvaji, S., Chattopadhyay, S., Inemella, S., Grandhi, V., Chigilipalli, Y., Puppala, Y. C., Sharma, M. H., Gubbala, S., Thakur, K., Aanaparthi, S., Pothula, B. and Yedidi, R.S. (2023). *In silico* analysis of molnupiravir usage vs. efficacy of COVID-19 vaccines. *TCABSE-J*, Vol. 1, Issue 5:1-11. Mar 22nd, 2023. Epub: Oct 20th, 2022.

Several vaccine strategies have been deployed to combat the recent pandemic caused by the coronavirus disease-2019 (COVID-19). According to the world health organization (WHO) more than 12 billion vaccine doses have been administered globally as of August, 2022. In spite of vaccinations the global cumulative number of deaths are close to 6.5 million as of August, 2022 since December 2019 (https://covid19.who.int/). Due to the advancements in the diagnostic methods, the global cumulative number of confirmed cases increased >12,000-fold as of January 2022 compared to January 2020. While Europe and the Americas were hard hit by COVID-19, the rest of the world equally contributed to the number of cases resulting in a global cumulative number of confirmed cases close to 0.6 billion thus qualifying COVID-19 as an ongoing pandemic as of August 2022 since December 2019. Owing to this perplexing epidemiological data from WHO mankind has witnessed the emergence of SARS CoV-2 variants from wild type, alpha, beta, etc. to omicron with constant changes in its genome challenging the existing vaccines (1). The viral spike protein (2) is critical in binding the human angiotensin converting enzyme-2 (ACE-2) receptor for viral entry into the host cell. Hence the viral spike protein is considered as a primary target (antigen) for vaccine design or passive immune therapies including plasma therapy. Besides huge efforts being put on vaccine development for COVID-19, development of antiviral agents gained equal importance. Among several small molecules, remdesivir, molnupiravir, favipiravir (inhibitors of viral replication by targeting the viral RNA-dependent RNA Polymerase, RdRp) were mainly focused on for clinical trials (3). These small molecules can be used in combination with other classes of drugs if needed (4). It has been shown that the latest omicron strain can also be treated successfully with these small molecules (5). Among these three antiviral agents, the mechanism of action for favipiravir is ambiguous (6), but both remdesivir (7) and molnupiravir (8, 9) have clear mechanisms of action i.e., slowing down or complete inhibition of viral replication by targeting the viral RdRp.

Molnupiravir is a small molecule (Molecular weight.: 329 Da) nucleoside-analog (10) with good oral bioavailability (11). As shown in Figure 1, molnupiravir is a prodrug that is activated intracellularly. The active ingredient in the prodrug, β-D-N4-Hydroxycytidine 5'-triphosphate (NHC- TP) that mimics cytidine and also its tautomeric form mimics uridine (12, 13). The human carboxylesterase-2 (CES-2) has been shown to activate the prodrug into active molnupiravir (NHC-TP) and that any genetic polymorphisms in CES-2 may affect the metabolism of NHC-TP (14). Normally during the emergence of SARS CoV-2 mutant variants, structure of the viral spike protein changes which may not only affect the efficacy of neutralizing antibodies (15) but also the viral fitness in parallel. Recently we have shown in a systematic study that mutations in the spike protein can lead to significant structural deviations posing threat to the efficacy of current vaccines (16, 17). As shown in Figure 2, molnupiravir is designed to generate mutations within the daughter strands of the viral RNA during the replication, escaping the proof-reading mechanism of the viral RdRp (18, 19). The resultant daughter strands of viral RNA may either contain mutations or encounter one of the three stop codons (UAG, UGA and UAA). The stop codons may result in truncated protein sequences i.e. truncated mutants of the viral spike protein. For example, as shown in Figure 3, we calculated that there is a possibility of 8 truncated mutants of the viral spike protein within the receptor binding domain (RBD) sequence (16) that was considered in this study. In spite of mutagenicity, carcinogenicity, teratogenicity and embryotoxicity (20), molnupiravir has been approved for COVID-19 treatment based on its antiviral activity in clinical trials (21-24) hoping for better management of the COVID-19 pandemic.

In this study, we hypothesized that the molnupiravir induced mutations or truncations in the viral spike protein may have severe damaging effects on the success of current vaccines. We performed a systematic computational analysis of the mRNA stability for various mutants including the truncated variants and compared this data with the resultant protein structural deviations in order to assess the damage that can be potentially caused to the efficacy of current vaccines. All calculations were performed using publicly available servers.

Materials & Methods:

Preparation of mutant RNA sequences: The nucleotide sequence for the RBD of wild type SARS-CoV-2 spike protein was taken as the working template as described previously (16). The entire nucleotide sequence containing 600 bases was divided into 200 triplet codons and the possible mutant nucleotide sequences (Figure 2) were listed based on the mutations that can be induced by molnupiravir for each codon separately (Table S1). During the replication cycle, molnupiravir causes mutations in the nucleotide sequence by replacing the nucleotides with either C's or U's (Figure 2). A set of mutant sequences were prepared systematically where each mutant sequence has a specific amino acid substitution or a stop codon (Table S2) in it. These mutant sequences were saved as separate files so that they can be copy-pasted into the online RNAfold web server.

RNAfold - energy calculations: The RNA secondary structures for mutants were generated along with the associated minimum free energy (MFE) values and ensemble diversity (ED) numbers using the RNAfold server

TCABSE-J Research Article
ISSN: 2583- 2557, *Volume 1, Issue 5, pp1-11. 2023.*

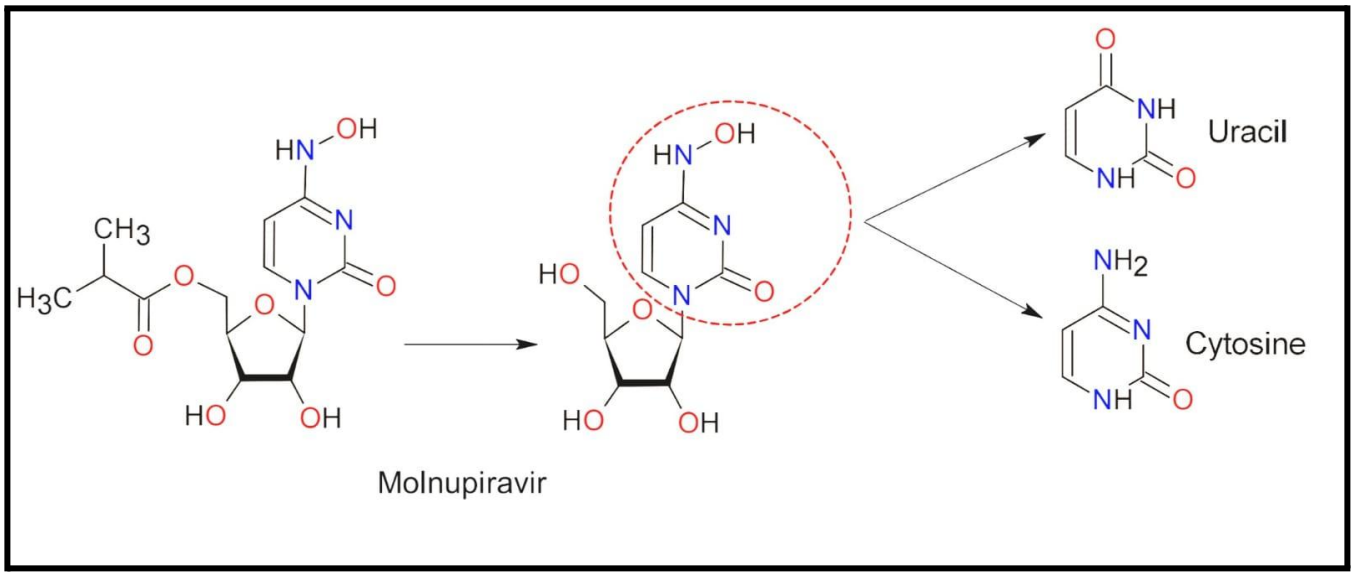

Figure 1. Activation mechanism of molnupiravir from its prodrug. The 5'-hydroxyl group is blocked in the prodrug form which is cleaved off and the phosphate groups are attached. The nitrogen base structure of molnupiravir mimics mostly with cytosine but its tautomeric form can also mimic uracil. This diagram was generated using ChemSketch software from ACD Labs.

(http://rna.tbi.univie.ac.at/cgi-bin/RNAWebSuite/RNAfold.cgi) (25-27) as previously described (16). Briefly, the mutant sequences were individually copy-pasted into the RNAfold web server and the results were downloaded. In order to compare the values, uniformity is maintained by dividing the MFE value of each mutant secondary structure by its corresponding ED number to obtain the average MFE (AMFE) values per iteration of the secondary structure ensemble. These AMFE values (Table S1) were then plotted in a multi-circular (MICI) plot as shown in Figure 4. This MICI plot also shows the correlations between AMFE values with protein structural deviations.

Generation of mutant protein models: Using the generated mutant RNA sequences above, corresponding amino acid sequences were manually generated as described previously (16). The mutant amino acid sequences were used for generating mutant protein models using the online SWISS MODEL web server (28, 29) as described previously (16). Briefly, mutant amino acid sequences were submitted to the online SWISS MODEL server and the resulting protein 3D model was downloaded.

Structural deviations: Structural deviations for mutant spike proteins were assessed based on the Root Mean Square Deviations (RMSDs) of Cα atomic positions as described previously (16, 17). Briefly, the mutant and wild type protein models generated using the SWISS MODEL server were superposed onto each other using LSQKAB program in the CCP4 (https://www.ccp4.ac.uk/) and resulting deviation at Cα atomic positions is noted (Table S3). The RMSDs were then plotted on the y-axis for the amino acid positions taken on the x-axis. The positions that show deviations below 5 Å are shown in Figure 4 (see top left small circle of MICI plot) and those that are above 5 Å are shown in Figure 5.

Protein-protein docking and binding affinity calculations: The protein models that have Cα RMSDs above 5 Å are superimposed onto the crystal structure containing spike protein RBD bound with ACE-2 receptor (PDB ID: 6M0J) one at a time using LSQKAB/CCP4. The mutant spike protein model built as described above and ACE-2 receptor of the 6M0J crystal structure are then considered for protein-protein docking using Rosie from Robetta server (https://rosie.rosettacommons. org/) (30). From the top 10 best scoring structures that are docked for each model that is given as input, the Interface Score (I_sc) of the first resultant structure (the highest score) is noted. I_sc gives the energy of interaction at the interface of spike protein RBD model and ACE-2 receptor. This can be considered as binding affinity (https://rosie.rosettacommons.org/docking2/documentation). Relative binding affinity of mutant protein models was obtained by dividing the binding affinity values of the mutant models with that of the wild type (Table S4).

Surface topology calculations for truncated mutants: Mutations induced by molnupiravir may result in stop codons at some positions generating truncated mutants (31) as shown in Figure 2 (see Tables S1 and S2 for further reference).

TCABSE-J Research Article
ISSN: 2583- 2557, *Volume 1, Issue 5, pp1-11. 2023.*

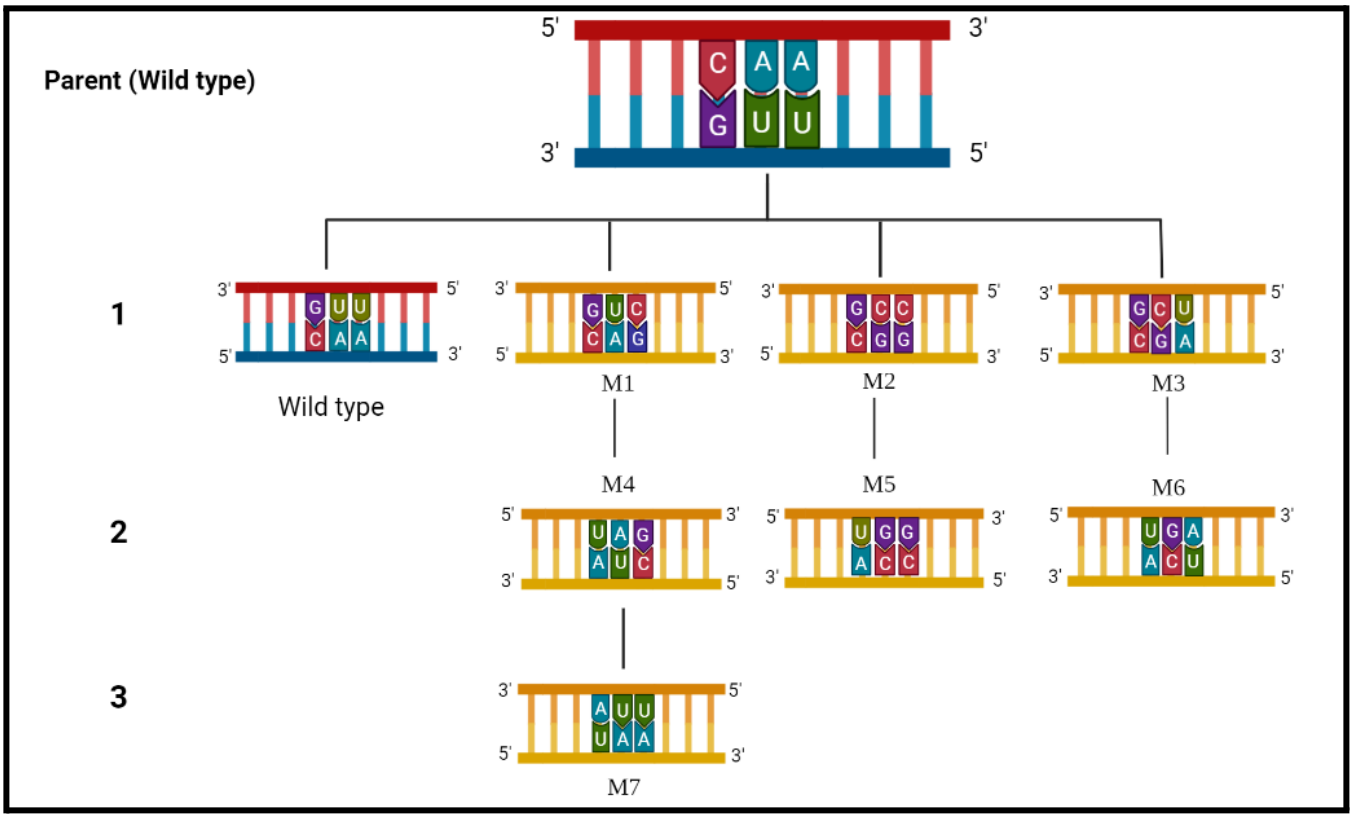

Figure 2. Site specific incorporation of molnupiravir tautomers mimicking either cytosine or uracil over 3 cycles of viral replication starting from the wild type parent RNA sequence CAA is shown here. Initially the complementary sequence of the parent strand (wild type) GUU can exist in 4 different combinations in the presence of molnupiravir viz. GUU, GUC, GCC and GCU. In the first round of replication, these 4 combinations give rise to CAA (wild type parent), CAG (mutant 1, M1), CGG (mutant 2, M2) and CGA (mutant 3, M3). In the second round of replication, M1 can also exist as M4 (UAG, stop codon); M2 can also exist as M5 (UGG) and M3 can also exist as M6 (UGA, stop codon). In the third round of replication, the M4 is capable of generating M7 (UAA, stop codon). Thus, in this particular wild type codon (CAA), there is a possibility of obtaining seven mutant codons (M1 to M7) of which three are stop codons (M4, M6 and M7) resulting in truncated proteins. Note: Stop codon incorporation does not affect viral replication but generates truncated proteins. This diagram was prepared using Biorender software.

Stop codons in a sequence lead to the termination of protein synthesis thereby resulting in truncated proteins with moderate to severe alterations in surface topology (16, 17). Determining the surface topology for truncated proteins is done by calculating the solvent accessible surface area using AreaiMol from CCP4 (https://www.ccp4.ac.uk/) as described previously (16, 17). The resultant surface area values were plotted in Figure 4 (see the top right small circle of the MICI plot).

PISA (Proteins, Interfaces, Structures and Assemblies) calculations: In order to understand the interface for the spike protein models that were generated above, the PISA (32-34) web server (https://www.ebi.ac.uk/pdbe/pisa/) was used. The coordinate file for each mutant was uploaded one at a time to the PISA server and the corresponding interface in terms of binding and assembly formation was calculated as the solvation free energy, ΔG kcal/mol. A total of 200 models were uploaded to the PISA server for the calculations as summarized in Table S5.

Results and Discussion:

Molnupiravir-induced mutant mRNA sequences show higher stability than wild type mRNAs: The viral spike protein expression levels are directly proportional to their corresponding mRNA stability i.e., the secondary structure of that particular mRNA sequence in the host cell cytoplasm. Hence we predicted the secondary structures of 1,401 mutant spike protein mRNA sequences (including the wild type) using RNAfold web server (http://rna.tbi.univie.ac.at/cgi-bin/RNAWebSuite/RNAfold.cgi) and plotted their average MFE (AMFE) values (see the RNAfold - energy calculations sections under the methods for details about AMFE calculations). As shown in the MICI plot in Figure 4, the big circle contains AMFE values of all the 1,401 mutants.

Figure 3. Multiple sequence alignment (MSA) showing all possible 8 truncated mutant protein sequences along with the position at which the stop codon was generated due to the site specific incorporation of molnupiravir. The sequence length of these truncated mutants range from 24 amino acids (W25STOP) to 177 amino acids (Q178STOP) when compared to the wild type which contains 200 amino acids covering the RBD of viral spike protein (16). This MSA was performed using CLUSTAL Ω.

The spike protein mRNA sequences are plotted in 7 concentric circles @ 200 mutants per circle. As shown in Figure 2, each triplet codon has a possibility to give rise to 7 mutants (including stop codons). Out of the 1,400 mutants, close to 560 mutants (~40%) showed higher AMFE values and 116 mutants (>8%) showed equal AMFE values compared to the wild type spike protein mRNA sequence, respectively (Figure 4). This analysis suggests that these mutant mRNAs might have an equal or better chance of survival in the host cell cytoplasm for longer periods of time and yield more mutant spike proteins, possibly outnumbering the wild type spike proteins. Excluding the above mentioned mutants, the remaining ~52% of the mutants have relatively lower AMFE values compared to the wild type spike protein mRNA thus supporting the antiviral activity of molnupiravir i.e. causing lethality to the virus. However, it is noteworthy that a given viral particle may not necessarily contain all wild type spike proteins on its surface but it may be a combination of both wild type and mutant viral spike proteins rather which creates heterogeneity. Such viral particles may or may not be successfully neutralized by the antibodies elicited by the current vaccines.

Structural deviations of substitution and truncated mutant spike protein models: Molnupiravir -induced base substitutions in the mRNA sequences lead to the production of mutant spike proteins that may either have amino acid substitutions or may be truncated due to a premature stop codon (Figures 2 and 3). Hence we analyzed the structural deviations of these mutant spike proteins by building their 3-dimensional models using SWISS MODEL web server. As detailed in Table S3, each triplet codon is capable of generating 7 different mutant codons due to the incorporation of molnupiravir (Figure 2). For example, the first codon in the sequence that was analyzed in this study at the 5'-end is "UUU" which codes for the amino acid F. In the presence of molnupiravir, this particular codon can also give rise to 7 mutant codons CUU, UCU, UUC, CCU, UCC, CUC & CCC.

ISSN: 2583- 2557, *Volume 1, Issue 5, pp1-11. 2023.*

TCABSE-J
Interdisciplinary Sciences Journal

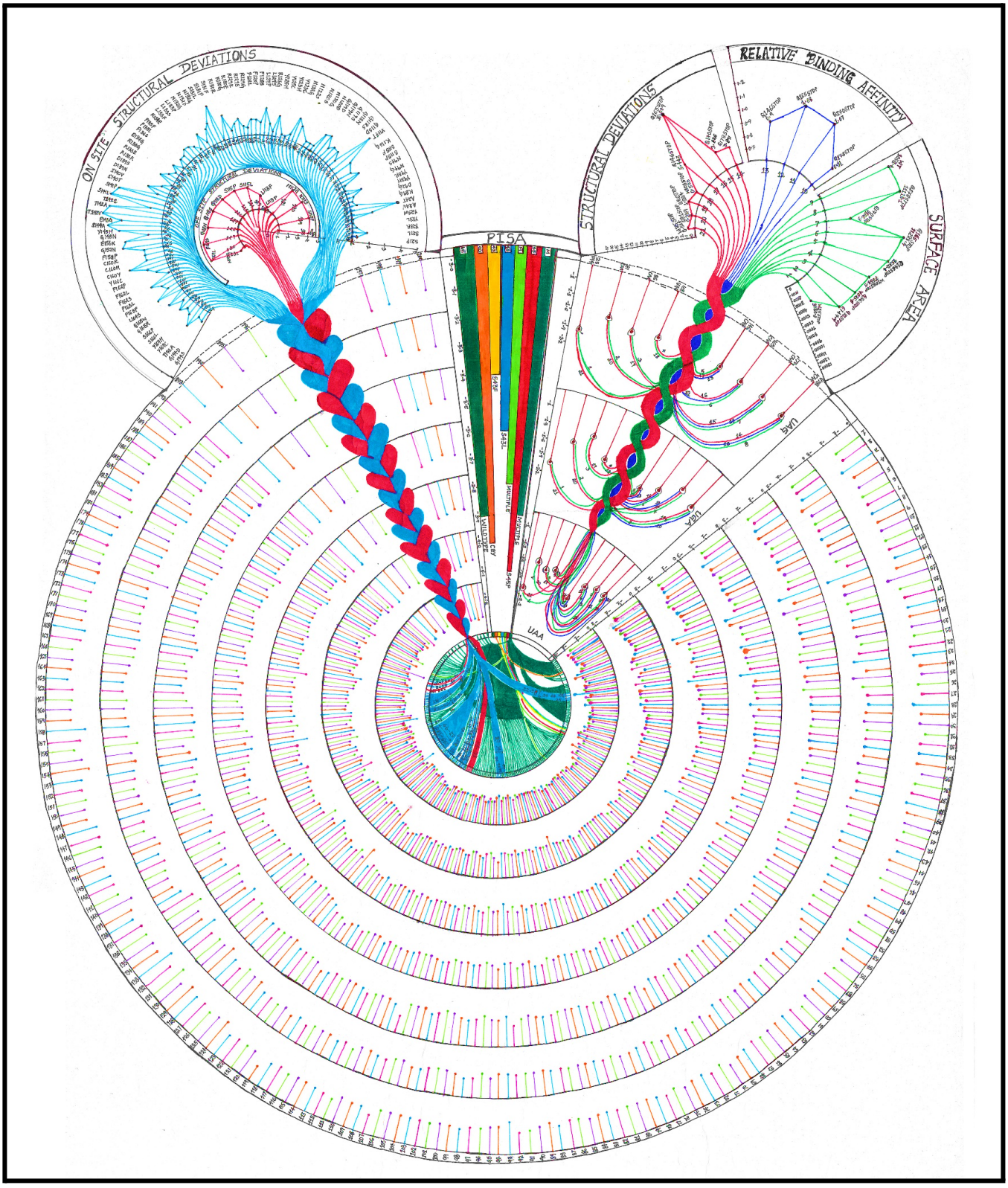

Figure 4. Multi-circular (MICI) plot showing the correlations among the mRNA AMFE values with protein structural deviations in molnupiravir induced mutants. This MICI plot contains three circles, one large circle (bottom) and two small circles (top left and top right). The large circle contains mRNA AMFE values for 1,400 molnupiravir-induced mutants plotted in 7 concentric circles with an inner circle filled with correlation lines from the top left small circle and PISA values plotted in the large circle between the two small circles on the top. The top left corner circle focuses on the structural deviations of 110 mutant spike protein models that have RMSDs between 1 Å and 4.99 Å (neglecting the truncated mutants). The inner circle (red color peaks) represents the offsite structural deviations for 14 mutants and the outer circle (cyan color peaks) represents the onsite structural deviations for 96 mutants. The RMSDs of 4 mutants (T142V, T142A, S141L & I144A) onsite and 6 mutants (S110P, S110F, N111S, N112G, F169S & F169L) offsite ranging from 4.4Å to 4.99Å are considered to be the highest among the 110 mutants. The mutants - S115P, G118D, G118S and G118N show both onsite and offsite RMSDs ranging 1 Å to 3.9 Å. The top right corner circle represents the data set corresponding to the stop codons of mutants, which is further divided into three sectors of Structural deviations (SDs), Relative binding affinities (RBAs) and surface area (SAs). It is observed that the molnupiravir induces stop codons (UAG, UGA and UAA) at eight positions (W25STOP, Q81STOP, Q86STOP, W108STOP, Q146STOP, Q165STOP, Q170STOP & Q178STOP) in the spike protein of SARS-CoV-2. The mutant strains Q165STOP and Q178STOP are observed to have more surface area in comparison with the wildtype spike protein. Out of the 8 stop codon mutants, only four of them (Q146, Q165, Q170 & Q178) are observed to have the highest binding affinities relative to wildtype spike protein. The Q165 mutant shows highest RMSD when superimposed with the wild type among all the 8 stop codons. The Q165 mutant is observed to be the highest in all the three sectors. The two knots coming out of the two small circles of the MICI plot are connected to the Average Minimum Free Energy (AMFE) values. There are 200 codons present in the wildtype spike protein of the SARs-CoV-2. There are seven concentric circles present in the major circle as each wildtype codon has 7 possible mutant codons. The mutants are represented with five different colors just to distinguish the set of codons from each other. PISA calculations are to estimate the total energy (measured in Kcal/mol) of mutant spike protein models which is based on crystallographic symmetry mates. Majority of the mutant models showed energy values between -3.8 kcal/mol and -3.9 kcal/mol with the wildtype value being -3.9 kcal/mol. However, the amino acid substitutions C8Y (-4.0 kcal/mol), S43F/L (-3.4/ -3.6 kcal/mol) and S45P (-4.1 kcal/mol) fall outside this range.

These mutant triplets code for the amino acids, L, S, F, P, S, L and P, respectively. Due to the codon redundancy (also known as degeneracy) multiple codons may code for a single amino acid which is evident in the repetition of the amino acids, L, S, F and P (Table S3). This suggests that at the first position (5'-end) of the sequence, there is a possibility of "F" being substituted with L/S/P/F only but not other amino acids. Based on this example, we prepared 606 mutant spike protein models (598 models containing amino acid substitutions + 8 truncated models due to premature stop codons) for the 200 triplet codons considered in this study instead of 1,400 models (200 triplets x 7 models per triplet = 1,400) to avoid any redundancy in our analysis. Similarly, out of 1,400 triplet codons, we obtained a total of 8 stop codons due to the incorporation of molnupiravir at positions W25, Q81, Q86, W108, Q146, Q165, Q170 and Q178. Evidently these stop codons are found replacing either Q (CAA, CAG) or W (UGG) because of the redundant nature of their triplet codons compared to stop codons UAA, UAG and UGA.

All the 606 mutant and truncated spike protein models were analyzed for their structural deviations i.e. their Cα RMSDs using the wild type spike protein model as the reference. Interestingly as reported previously by our group (16, 17) we observed major structural deviations in the mutant/truncated models both at the site of mutation (onsite) and away from the site of mutation (offsite). As shown in Figure 5, the major onsite and offsite RMSDs of 152 mutants (out of 606 mutant models, 25%) containing amino acid substitutions range from 10 Å to >20 Å and 23 mutants (out of 606 mutant models, ~4%) show RMSDs between 5 Å and 10 Å. As shown in Figure 6, four mutant spike proteins containing amino acid substitutions showed major RMSDs. Major RMSDs are: Y125H (onsite: 2.4 Å and offsite: 21.9 Å at position N153), S131L (onsite: 2.5 Å and offsite: 22.6 Å at position G154), T150V (onsite: 15.325 Å and offsite: 23.8 Å at position G148) and E156G (onsite: 20.8 Å and offsite: 22.0 Å at position V155). RMSDs that were <1 Å were considered insignificant (see top left small circle in Figure 4) owing to the errors in model building algorithms. Four out of 8 truncated mutant spike protein models generated due to premature stop codons showed RMSDs >3 Å. As shown in Figure 4 (see top right small circle) the truncations Q146STOP and Q165STOP exhibited the highest RMSDs of 5.4 Å and 16.0 Å, respectively while the Q170STOP and Q178STOP each showed an RMSD value of <4 Å (Table S2). All RMSDs for the truncated mutants were seen offsite. Onsite RMSDs were not calculated due to the truncation. Thus, the structural deviations presented in this study contribute to significant changes in the antigen topology posing threat to the neutralizing antibodies that are generated by current vaccines and these RMSDs should be considered carefully in future vaccine design in order to increase their efficacy. However, molnupiravir-induced mutants with significant structural deviations may also prove to be lethal for the survival of the mutant virus in addition to challenging the efficacy of current vaccines. In order to further dissect this dilemma, we investigated the binding affinities of the mutant spike protein models (with high RMSDs) against the human ACE-2 receptor.

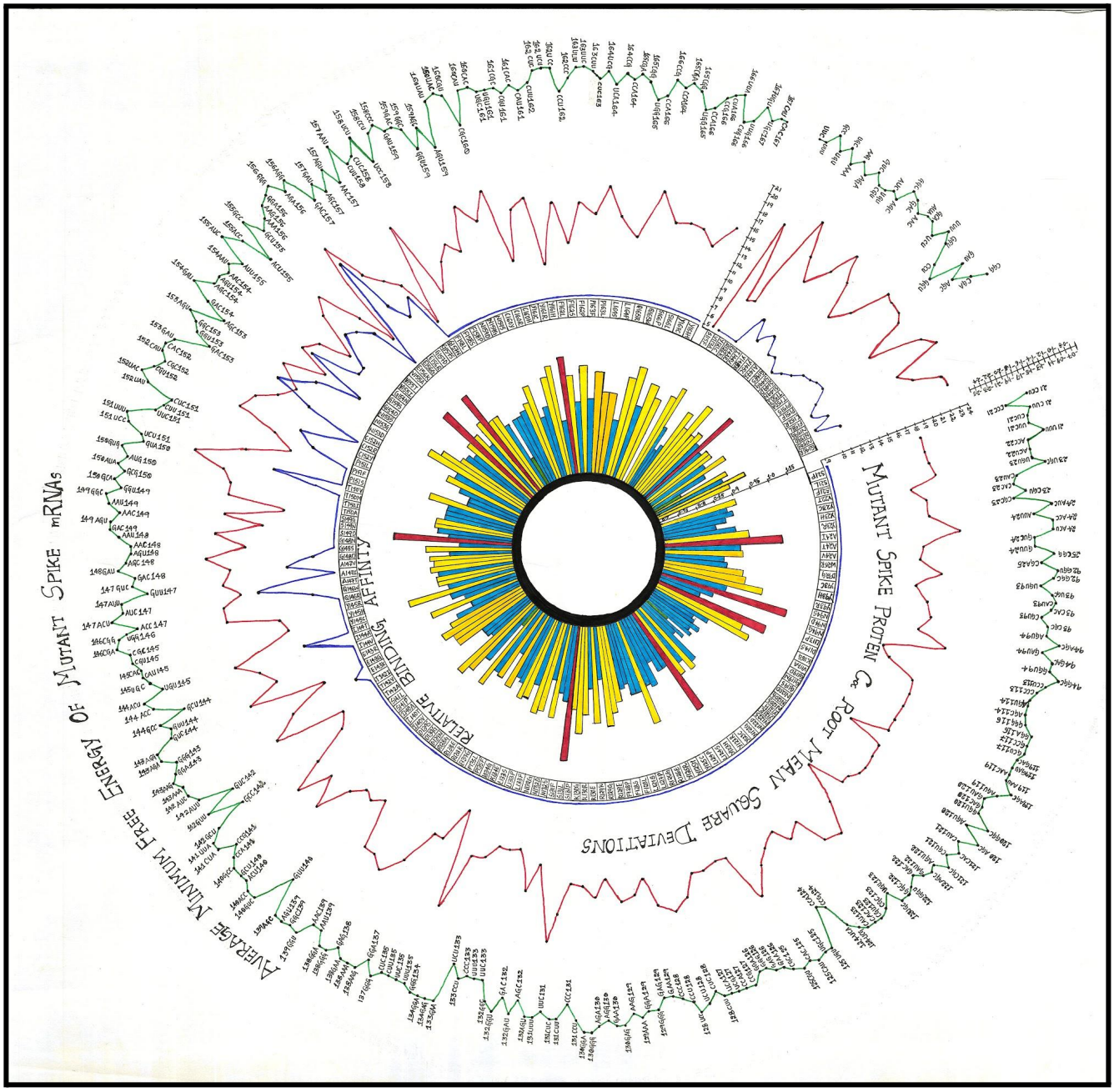

Figure 5. Circular plot showing the structural deviations (>5) in molnupiravir induced mutant spike protein models compared to the wild type spike protein model. The outermost circle of the circular plot contains the average minimum free energy values ranging from -0.7 kcal/mol to -2.5 kcal/mol. The center circle consists of 305 codons that code for the mutant spike proteins that are showing the structural deviations above 5Å, out of which a small sector towards the top right corner shows less than 5Å. Three codons have onsite deviations below 5Å deviations & offsite deviations between 5Å-10Å. The total of 19 codons has onsite deviations between 5Å-10Å where the offsite deviations are above 10Å. The other 302 codons have the offsite deviations of above 10Å, out of which 23 codons have onsite deviations of above 10Å. The innermost circle consists of relative binding affinities (RBA) [RBA= binding affinity (BA) of the mutant spike protein / binding affinity of the wildtype spike protein] of mutant spike proteins (MSPs) towards the ACE2 receptor; there are three MSPs (Y121H, D139G & F158L) with RBA of 0.7 to 0.79 which are considered as the least RBA binding affinity and there are nine MSPs (A24I, N94D, D114S, Y123H, S131L, S149D, V155T, E156R & Y161H) with RBA of 1.0 to 1.99 which are considered as the highest RBA. While the rest of the 140 MSPs have the moderate binding affinities.

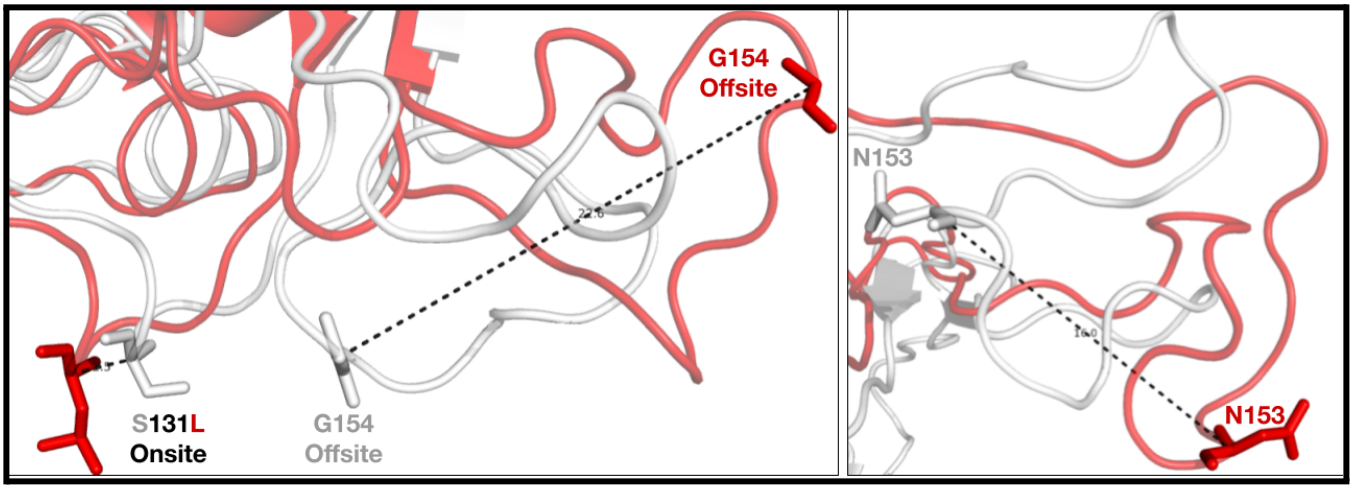

Figure 6. Major structural deviations in mutants with amino acid substitutions (left panel) and truncated mutants with premature stop codon (right panel). In both panels the wild type and mutant spike protein models are shown in white color and red color, respectively. In the left panel, the amino acid substitution (Ser to Leu) at position 131 resulted in an RMSD of 2.5 Å (onsite) and 22.6 Å at G154 (offsite). In the right panel the stop codon at position 165 (not shown here) resulted in an RMSD of 16 Å at N153 (offsite).

Binding affinities: Considering the significant structural deviations in the mutant spike protein models discussed above, we further evaluated their binding affinities against the human ACE-2 receptor by using the Rosie protein-protein docking from Rosetta web server. Our focus was mainly on the mutant spike protein models that showed >5 Å RMSDs (Figure 5). Among the 175 mutants containing amino acid substitutions plotted in Figure 5, nine of them (A24I, N94D, D114S, Y123H, S131L, S149D, V155T, E156R & Y161H) exhibited reasonable binding affinity that is either comparable or better than the binding affinity of wild type spike protein against the human ACE-2 receptor. Among the 8 truncated mutants of the spike protein, only two (Q165STOP and Q170STOP) showed reasonable binding affinities (see top right small circle in Figure 4) that are either comparable or better than the binding affinity of wild type spike protein against human ACE-2 receptor. The Rosie docking did not work for 4 of the truncated mutants, W25STOP, Q81STOP, Q86STOP and W108STOP partially indicating that they could be lethal for the virus. Our current data analysis suggests that out of all possible mutant and truncated variants of spike protein models that can be generated due to the incorporation of molnupiravir, a total of 11 (9 substitution mutants and 2 truncated mutants) can bind the human ACE-2 receptor with reasonable binding affinities that are comparable or better than the binding affinity of the wild type spike protein. These variants, if survive and replicate successfully, then there is a high chance of risk to the efficacy of current vaccines owing to the fact that a single viral particle may contain heterogeneously distributed spike proteins on its surface that are a mix of wild type, mutants and trucations.

Decrease in surface area of truncated mutants explains loss of binding affinity: Our study demonstrates the possibility of 8 stop codons into the viral mRNA during the viral replication in the presence of molnupiravir (Figures 2 and 3). Among the 8 truncated spike protein models, 3 of them (W25STOP, Q81STOP and Q86STOP) show >50% loss of the total protein length. Hence we analyzed the total solvent accessible surface area of these truncated mutants in comparison to the full length wild type (16). As shown in Figure 4 (top right small circle) the total surface area for each of these 3 truncated mutants is at least 1.5- to 3.5-fold lower than the surface area of wild type. The significant decrease in the surface area explains loss of binding affinity for these 3 truncated mutants against the human ACE-2 receptor thus posing a lethal threat for the survival of the virus. However, the truncated mutant Q165STOP showed more surface area than wild type and also this particular truncated mutant spike protein showed increased binding affinity than wild type spike protein against human ACE-2 receptor suggesting that it could be a threat to the efficacy of current vaccines. Additionally, the changes in surface area could also contribute to the changes in the topology of the antigen (spike protein) thus altering the epitopes for the neutralizing antibodies.

We further performed interface calculations for wild type and mutant spike protein models using the PISA web server (https://www.ebi.ac.uk/ pdbe/pisa/). As shown in Figure 4, the majority of mutant spike protein models showed comparable calculated solvation free energy (ΔG kcal/mol.) values with the wild type spike protein model indicating that they are capable of interacting with ACE-2

receptor and that they are also capable of forming assemblies with other interacting proteins. Out of 590 mutant models (Table S5), the C8Y and S45P substitutions showed slightly better solvation free energy (ΔG kcal/mol.) while mutant models S43F and S43L showed lower solvation free energy (ΔG kcal/mol.) compared to the wild type. The remaining 99% of the models showed solvation free energy values either equal (-3.9 kcal/mol.) or almost equal (-3.8 kcal/mol) to the solvation free energy of the wild type spike protein model (-3.9 kcal/mol.). This finding suggests that 99% of mutant spike protein models that were generated in this study behave normally with respect to the wild type spike protein models for physiological purposes such as the spike protein trimer formation. If such molnupiravir-induced mutant spike protein models can camouflage the wild type then the success of current vaccines is at risk.

Conclusion: Taken together, our studies provide substantial insights into the lethal effects of molnupiravir usage on the success and efficacy of current vaccines. However, our hypothesis makes an assumption that such vaccine failure is only possible if the mutant variants of SARS CoV-2 generated due to the incorporation of molnupiravir can survive and successfully replicate (e.g., the truncated mutant, Q165STOP). Further, this study is exclusively focused on the viral spike protein but molnupiravir-induced mutations may also occur in other viral proteins such as the viral RdRp that is responsible for proofreading the viral transcripts during replication. Functional mutants of RdRp with lost proofreading mechanism may pose a severe threat to the current vaccines either in the presence or absence of molnupiravir in future thus fueling the emergence of lethal viral strains that could be hard to treat even with the antivirals such as paxlovid (35). Although our efforts were focused on balancing the synergistic and catastrophic effects of molnupiravir co-administered with vaccination, our results point more towards the catastrophe rather than synergy. Our current *in silico* studies, however, require further validations through appropriate *in vitro* and *in vivo* experiments in the future. We are currently comparing the mutants from this study with corresponding clinical data from hospitals.

Acknowledgements:
We thank The Yedidi Institute for Discovery and Education (TyiDE-Toronto) for funding the work presented in this article and also for helping us writing and editing the manuscript to its final version.

Conflict of interest: The authors declare no conflict of interest in this study. However, this research article is an ongoing project currently at TCABS-E, Visakhapatnam, India.

References

1. Fang FF, Shi PY. Omicron: a drug developer's perspective. *Emerg Microbes Infect*. 2022 Dec;11(1):208-211. doi: 10.1080/22221751.2021.2023330.
2. Xia X. Domains and Functions of Spike Protein in Sars-Cov-2 in the Context of Vaccine Design. *Viruses*. 2021 Jan 14;13(1):109. doi: 10.3390/v13010109.
3. Vangeel L, Chiu W, De Jonghe S, Maes P, Slechten B, Raymenants J, André E, Leyssen P, Neyts J, Jochmans D. Remdesivir, Molnupiravir and Nirmatrelvir remain active against SARS-CoV-2 Omicron and other variants of concern. *Antiviral Res.* 2022 Feb;198:105252. doi: 10.1016/j.antiviral.2022.105252.
4. Wang X, Sacramento CQ, Jockusch S, Chaves OA, Tao C, Fintelman-Rodrigues N, Chien M, Temerozo JR, Li X, Kumar S, Xie W, Patel DJ, Meyer C, Garzia A, Tuschl T, Bozza PT, Russo JJ, Souza TML, Ju J. Combination of antiviral drugs inhibits SARS-CoV-2 polymerase and exonuclease and demonstrates COVID-19 therapeutic potential in viral cell culture. Commun Biol. 2022 Feb 22;5(1):154. doi: 10.1038/s42003-022-03101-9.
5. Li P, Wang Y, Lavrijsen M, Lamers MM, de Vries AC, Rottier RJ, Bruno MJ, Peppelenbosch MP, Haagmans BL, Pan Q. SARS-CoV-2 Omicron variant is highly sensitive to molnupiravir, nirmatrelvir, and the combination. *Cell Res*. 2022 Mar;32(3):322-324. doi: 10.1038/s41422-022-00618-w.
6. Jin Z, Smith LK, Rajwanshi VK, Kim B, Deval J (2013) The Ambiguous Base-Pairing and High Substrate Efficiency of T-705 (Favipiravir) Ribofuranosyl 5′-Triphosphate towards Influenza A Virus Polymerase. *PLoS ONE* 8(7): e68347. https://doi.org/10.1371/journal.pone.0068347
7. Cho A, Saunders OL, Butler T, Zhang L, Xu J, Vela JE, Feng JY, Ray AS, Kim CU. Synthesis and antiviral activity of a series of 1'-substituted 4-aza-7,9-dideazaadenosine C-nucleosides. *Bioorg Med Chem Lett.* 2012 Apr 15;22(8):2705-7. doi: 10.1016/j.bmcl.2012.02.105.
8. Swanstrom R, Schinazi RF. Lethal mutagenesis as an antiviral strategy. *Science*. 2022 Feb 4;375(6580):497-498. doi: 10.1126/science.abn0048.
9. Masyeni S, Iqhrammullah M, Frediansyah A, Nainu F, Tallei T, Emran TB, Ophinni Y, Dhama K, Harapan H. Molnupiravir: A lethal mutagenic drug against rapidly mutating severe acute respiratory syndrome coronavirus 2-A narrative review. J Med Virol. 2022 Jul;94(7):3006-3016. doi: 10.1002/jmv.27730.
10. Toots M, Yoon JJ, Cox RM, Hart M, Sticher ZM, Makhsous N, Plesker R, Barrena AH, Reddy PG, Mitchell DG, Shean RC, Bluemling GR, Kolykhalov AA, Greninger AL, Natchus MG, Painter GR, Plemper RK. Characterization of orally efficacious influenza drug with high resistance barrier in ferrets and human airway epithelia. Sci Transl Med. 2019 Oct 23;11(515):eaax5866. doi: 10.1126/scitranslmed.aax5866.
11. Whitley R. Molnupiravir - A Step toward Orally Bioavailable Therapies for Covid-19. *N Engl J Med*. 2022 Feb 10;386(6):592-593. doi: 10.1056/NEJMe2117814.
12. Malone B, Campbell EA. Molnupiravir: coding for catastrophe. *Nat Struct Mol Biol.* 2021 Sep;28(9):706-708. doi: 10.1038/s41594-021-00657-8.
13. Painter WP, Holman W, Bush JA, Almazedi F, Malik H, Eraut NCJE, Morin MJ, Szewczyk LJ, Painter GR. Human Safety, Tolerability, and Pharmacokinetics of Molnupiravir, a Novel Broad-Spectrum Oral Antiviral Agent with Activity Against

SARS-CoV-2. *Antimicrob Agents Chemother.* 2021 Mar 1;65(5):e02428-20. doi: 10.1128/AAC.02428-20.
14. Shen Y, Eades W, Liu W, Yan B. The COVID-19 oral drug molnupiravir is a CES2substrate: potential drug-drug interactions and impact of CES2 genetic polymorphism in vitro. *Drug Metab Dispos.* 2022 Jul 5:DMD-AR-2022-000918. doi: 10.1124/dmd.122.000918.
15. Finkelstein MT, Mermelstein AG, Parker Miller E, Seth PC, Stancofski ED, Fera D. Structural Analysis of Neutralizing Epitopes of the SARS-CoV-2 Spike to Guide Therapy and Vaccine Design Strategies. *Viruses*. 2021 Jan 19;13(1):134. doi: 10.3390/v13010134.
16. Addala S, Vissapragada M, Aggunna M, Mukala N, Lanka M, Gampa S, Sodasani M, Chintalapati J, Kamidi A, Veeranna RP, Yedidi RS. Success of Current COVID-19 Vaccine Strategies vs. the Epitope Topology of SARS-CoV-2 Spike Protein-Receptor Binding Domain (RBD): A Computational Study of RBD Topology to Guide Future Vaccine Design. *Vaccines* (Basel). 2022 May 25;10(6):841. doi: 10.3390/vaccines10060841.
17. Vissapragada M, Addala S, Sodasani M, Yedidi RS. Major structural deviations in the receptor binding domain of SARS-CoV-2 spike protein may pose threat to the existing vaccines. *TCABSE-J* 2021. Apr 13th; 1(1):12-14.
18. Hashemian SMR, Pourhanifeh MH, Hamblin MR, Shahrzad MK, Mirzaei H. RdRp inhibitors and COVID-19: Is molnupiravir a good option? *Biomed Pharmacother.* 2022 Feb;146:112517. doi: 10.1016/j.biopha.2021.112517.
19. Hadj Hassine, I., Ben M'hadheb, M., & Menéndez-Arias, L. (2022). Lethal Mutagenesis of RNA Viruses and Approved Drugs with Antiviral Mutagenic Activity. *Viruses*, *14*(4), 841. https://doi.org/10.3390/v14040841.
20. Waters MD, Warren S, Hughes C, Lewis P, Zhang F. Human genetic risk of treatment with antiviral nucleoside analog drugs that induce lethal mutagenesis: The special case of molnupiravir. *Environ Mol Mutagen*. 2022 Jan;63(1):37-63. doi: 10.1002/em.22471.
21. Vena, A., Traman, L., Bavastro, M., Limongelli, A., Dentone, C., Magnè, F., Giacobbe, D. R., Mikulska, M., Taramasso, L., Di Biagio, A., & Bassetti, M. (2022). Early Clinical Experience with Molnupiravir for Mild to Moderate Breakthrough COVID-19 among Fully Vaccinated Patients at Risk for Disease Progression. *Vaccines*, *10*(7), 1141. https://doi.org/10.3390/vaccines10071141.
22. Tian, L., Pang, Z., Li, M., Lou, F., An, X., Zhu, S., Song, L., Tong, Y., Fan, H., & Fan, J. (2022). Molnupiravir and Its Antiviral Activity Against COVID-19. *Frontiers in immunology*, *13*, 855496. https://doi.org/10.3389/fimmu.2022.855496.
23. Agostini, M. L., Pruijssers, A. J., Chappell, J. D., Gribble, J., Lu, X., Andres, E. L., Bluemling, G. R., Lockwood, M. A., Sheahan, T. P., Sims, A. C., Natchus, M. G., Saindane, M., Kolykhalov, A. A., Painter, G. R., Baric, R. S., & Denison, M. R. (2019). Small-Molecule Antiviral β-d-*N*4-Hydroxycytidine Inhibits a Proofreading-Intact Coronavirus with a High Genetic Barrier to Resistance. *Journal of virology*, *93*(24), e01348-19. https://doi.org/10.1128/JVI.01348-19.
24. Jayk Bernal, A., Gomes da Silva, M. M., Musungaie, D. B., Kovalchuk, E., Gonzalez, A., Delos Reyes, V., Martín-Quirós, A., Caraco, Y., Williams-Diaz, A., Brown, M. L., Du, J., Pedley, A., Assaid, C., Strizki, J., Grobler, J. A., Shamsuddin, H. H., Tipping, R., Wan, H., Paschke, A., Butterton, J. R., Johnson, M. G., De Anda C., MOVe-OUT Study Group (2022). Molnupiravir for Oral Treatment of Covid-19 in Nonhospitalized Patients. *The New England journal of medicine*, *386*(6), 509–520. https://doi.org/10.1056/NEJMoa2116044.
25. Gruber AR, Lorenz R, Bernhart SH, Neuböck R, Hofacker IL. The Vienna RNA Websuite. Nucleic Acids Research, Volume 36, Issue suppl_2, 1 July 2008, Pages W70-W74, DOI: 10.1093/nar/gkn188
26. Lorenz, R. and Bernhart, S.H. and Höner zu Siederdissen, C. and Tafer, H. and Flamm, C. and Stadler, P.F. and Hofacker, I.L. "ViennaRNA Package 2.0", Algorithms for Molecular Biology, 6:1 page(s): 26, 2011
27. Mathews DH, Disney MD, Childs JL, Schroeder SJ, Zuker M, Turner DH. (2004) Incorporating chemical modification constraints into a dynamic programming algorithm for prediction of RNA secondary structure. *Proc Natl Acad Sci U S A* 101(19):7287-92.
28. Waterhouse A, Bertoni M, Bienert S, Studer G, Tauriello G, Gumienny R, Heer FT, de Beer TAP, Rempfer C, Bordoli L, Lepore R, Schwede T. SWISS-MODEL: homology modelling of protein structures and complexes. *Nucleic Acids Res*. 2018 Jul 2;46(W1):W296-W303. doi: 10.1093/nar/gky427.
29. Bienert S, Waterhouse A, de Beer TA, Tauriello G, Studer G, Bordoli L, Schwede T. The SWISS-MODEL Repository-new features and functionality. *Nucleic Acids Res*. 2017 Jan 4;45(D1):D313-D319. doi: 10.1093/nar/gkw1132.
30. Sergey Lyskov, Jeffrey J. Gray, The RosettaDock server for local protein–protein docking, *Nucleic Acids Research*, Volume 36, Issue suppl_2, 1 July 2008, Pages W233–W238, https://doi.org/10.1093/nar/gkn216.
31. Kabinger, F., Stiller, C., Schmitzová, J. *et al.* Mechanism of molnupiravir-induced SARS-CoV-2 mutagenesis. *Nat Struct Mol Biol* 28, 740–746 (2021). https://doi.org/10.1038/s41594-021-00651- 0.
32. Krissinel, E., & Henrick, K. (2007). Inference of macromolecular assemblies from crystalline state. *Journal of molecular biology*, *372*(3), 774–797. https://doi.org/10.1016/j.jmb.2007.05.022
33. Krissinel, E., Henrick, K. (2005). Detection of Protein Assemblies in Crystals. In: R. Berthold, M., Glen, R.C., Diederichs, K., Kohlbacher, O., Fischer, I. (eds) Computational Life Sciences. CompLife 2005. Lecture Notes in Computer Science(), vol 3695. Springer, Berlin, Heidelberg. https://doi.org/10.1007/11560500_15
34. Krissinel E. (2010). Crystal contacts as nature's docking solutions. *Journal of computational chemistry*, *31*(1), 133–143. https://doi.org/10.1002/jcc.21303
35. Owen, D. R., Allerton, C., Anderson, A. S., Aschenbrenner, L., Avery, M., Berritt, S., Boras, B., Cardin, R. D., Carlo, A., Coffman, K. J., Dantonio, A., Di, L., Eng, H., Ferre, R., Gajiwala, K. S., Gibson, S. A., Greasley, S. E., Hurst, B. L., Kadar, E. P., Kalgutkar, A. S., … Zhu, Y. (2021). An oral SARS-CoV-2 Mpro inhibitor clinical candidate for the treatment of COVID-19. *Science (New York, N.Y.)*, *374*(6575), 1586–1593. https://doi.org/10.1126/science.abl4784.